Battery Technologies for Large-Scale Stationary Energy Storage

Grigorii L. Soloveichik

General Electric Global Research, Niskayuna, New York 12309; email: soloveichik@ge.com

Annu. Rev. Chem. Biomol. Eng. 2011. 2:503–27

First published online as a Review in Advance on March 23, 2011

The *Annual Review of Chemical and Biomolecular Engineering* is online at chembioeng.annualreviews.org

This article's doi:
10.1146/annurev-chembioeng-061010-114116

1947-5438/11/0715-0503$20.00

Keywords

electrochemistry, secondary battery, fuel cell

Abstract

In recent years, with the deployment of renewable energy sources, advances in electrified transportation, and development in smart grids, the markets for large-scale stationary energy storage have grown rapidly. Electrochemical energy storage methods are strong candidate solutions due to their high energy density, flexibility, and scalability. This review provides an overview of mature and emerging technologies for secondary and redox flow batteries. New developments in the chemistry of secondary and flow batteries as well as regenerative fuel cells are also considered. Advantages and disadvantages of current and prospective electrochemical energy storage options are discussed. The most promising technologies in the short term are high-temperature sodium batteries with β''-alumina electrolyte, lithium-ion batteries, and flow batteries. Regenerative fuel cells and lithium metal batteries with high energy density require further research to become practical.

INTRODUCTION

The very nature of electricity generation, distribution, and usage requires a method to balance supply and demand. The simplest way to solve this problem is to store energy in some form when the demand is low and to return it to the electric grid when the demand is high. Implementation of large-scale electric energy storage (EES) will avoid the building of excessive energy generation capacity to meet short-term peak demand for electricity. Based on an analysis by the U.S. Department of Energy (DOE), EES should be approximately 1.7% of new generation capacity to minimize the effect of the system's variability (1). In addition, stationary energy storage is a key enabler for the smart grid concept and for wide implementation of intermittent renewable energy sources such as solar and wind.

Several different types of energy storage can be used for large-scale stationary applications, namely mechanical, electrical, chemical, and electrochemical (**Table 1**). The Electricity Storage Association (ESA; **http://www.electricitystorage.org**) identified twelve specific energy storage technologies based on these four types of energy storage. Examples of mechanical energy storage systems are flywheels, pumped-storage hydroelectricity (also known as pumped hydro), and compressed air energy storage (CAES). Electrical energy storage systems are based on supercapacitors and superconductive electromagnetic storage. An example of chemical storage is the energy stored in the form of hydrogen or other chemicals. Secondary (rechargeable) and redox flow batteries (in which a solution of one or more electroactive species flows through an electrochemical cell) as well as regenerative fuel cells, which can be operated both in direct and reverse (consuming electricity and producing energy rich chemicals), are examples of electrochemical energy storage.

Table 1 Energy storage technologies for stationary applications

Technology	Typical power, MW	Discharge time	Storage capacity cost, $ kWh^{-1}	Life time, cycle/years	Efficiency, %	Drawbacks
Flywheels	1	<5 min	1,000–2,000	100,000/>10	>90	Cost, power applications
Compressed air energy storage (CAES)	2,700	2–10 h	90–200	>5,000/>10	50	Site specific, storage and transmission cost
Pumped-storage hydroelectricity (pumped hydro)	4,000 (up to 22,500)	4–12 h	75–100	>10,000/>25	75–80	Site specific, transmission cost, environment
Supercapacitors	0.25	<1 min	500–3,000	500,000/20	>90	Explosion hazard, low energy density, cost
Superconductive electromagnetic storage (SMES)	10[a]	1–30 min	2,000–10,000	100,000/20	97	High capital cost, cryogenics
Chemical (hydrogen)	10[a]	>5 h		13	40–50	Low density storage, high cost, safety
Secondary batteries (lead-acid, Li-ion, NAS)	0.5–1	1–8 h	250–3,500	1,000–4,500/7–20	75–80	High cost, low cycle life
Flow battery (vanadium redox battery)	12	10 h	150–2,500	500–2,000/10	70	Low energy density

[a] Projected.

Several reviews comparing different energy storage options for stationary applications have been published recently (2–9).

This review gives an overview of the past ten years of progress in electrochemical storage methods at different stages of development, from mature technologies to emerging technologies to new chemistries.

APPLICATIONS

Utility-scale applications of energy storage are both energy related, such as peak shaving (0.1–10 MW), load leveling (1–100 MW), and energy arbitrage (50–500 MW), and power related, such as frequency and voltage regulation (spinning reserve), power quality regulation, and bridging power (1–30 MW) (10). The necessary response times for energy storage vary from seconds in power quality applications to hours for energy management applications. In addition, it is anticipated that increased market penetration of intermittent renewable energy sources (solar and wind) will require their smooth integration into the power grid and enable advanced smart grid operations. Commercial electrochemical energy storage systems have 100 kW to 20 MW of power and from 50 kWh to 40 MWh of energy capacity (7). For telecommunications (telecom) applications, EES needs several hours of operation to balance electricity supply outages. In contrast, for uninterruptible power supply (UPS) systems, which are usually smaller than 500 kW, an EES system must supply very high currents over short times (minutes) until the backup system responds. Safety, reliability, and durability are the most important criteria for stationary applications. Multi-MW systems must be built as turnkey systems, whereas smaller systems may be developed as modular ones.

Grid-scale stationary EES system revenues are expected to grow from $1.5 billion in 2010 to $25.3 billion over the next 10 years, according to a new report from Pike Research (11). Pike predicts that the most significant growth will be in CAES, Li-ion batteries, and flow batteries. Although only lead-acid batteries currently meet cost targets for EES, it is anticipated that flow batteries and high-temperature sodium batteries will increase their market share (12).

SECONDARY BATTERIES

A secondary battery, also known as rechargeable or storage battery, is a group of electrically connected electrochemical cells based on reversible electrochemical reactions. During the charge process, the anode active material is oxidized to generate electrons, and the cathode active material is reduced, which consumes electrons flowing through the external circuit. The charge balance is provided by ion flow between electrodes through an ion-conducting electrolyte. During the discharge process, these processes run backward. In secondary batteries, at least one of the active materials is present in a solid state.

Mature Technologies

Several battery technologies have been in use long enough to be considered mature technologies. These batteries, such as lead-acid, nickel-cadmium, and nickel-metal hydride, are produced by multiple manufacturers in different sizes for different stationary applications.

Lead-acid batteries. The lead-acid secondary battery was invented in 1859 by Gaston Planté and is based on simple chemistry (Equation 1):

$$\mathrm{Pb} + \mathrm{PbO_2} + 2\,\mathrm{H_2SO_4} \Leftrightarrow 2\,\mathrm{PbSO_4} + 2\,\mathrm{H_2O} \qquad E^0 = 2.04\ \mathrm{V}. \qquad 1.$$

The mature lead-acid battery technology is widely used in many mobile and stationary applications. For stationary applications, the valve-regulated lead-acid (VRLA) battery is the battery of choice but, to lesser extent, traditional flooded batteries are also used. The VLRA battery, also known as the sealed lead-acid battery, uses the recombination of the oxygen evolved at the positive plates with the hydrogen evolved on the negative plates, thus generating water and eliminating the requirement for water addition in the traditional lead-acid battery.

Some recent improvements in lead-acid battery technology were aimed at automotive applications but could be used in stationary batteries as well. For example, it was found that the solid lead anode could be partially replaced with carbon to convert it into a battery-supercapacitor hybrid named the UltraBattery (13–16). In addition, Kelley & Votoupal (17) proposed a corrosion-resistant current collector made of high–surface area carbon foam. This technology was used by FireFly Energy to develop lighter batteries with higher energy density, but the company went out of business in March 2010. In other research, coating lead plates with a thin layer of graphite prevented sulfation of the negative plate (18).

Pure lead electrodes are not sufficiently mechanically strong that they can be made big enough for large-scale applications, and they cannot tolerate high currents. Lead-antimony alloys display better corrosion resistance and can be made into taller plate designs, but they are not suitable for standby applications because of antimony poisoning. Addition of selenium and other elements to lead-antimony alloys overcomes this deficiency (19).

Recent advances in lead-acid batteries are associated with development of new gel electrolytes and separators (20, 21). For example, in VRLA batteries a novel polysiloxane-based gel electrolyte with an open 3D network structure showed higher discharge capacity and better temperature tolerance than the traditional fumed-silica gel electrolyte (22).

Both flooded and valve-regulated lead-acid cells are used in large-scale EES installations for UPS, peak shaving, and voltage and frequency control (500 kW–20 MW/500 kWh–40 MWh). Key manufacturers are Exide Technologies (**http://www.exide.com**), C&D Battery (**http://www.cdpowercom.com**), Hagen Batterie AG (**http://www.hagen-batterie.de**), and Storage Battery Systems (**http://www.sbsbattery.com**).

Nickel-cadmium batteries. Alkaline NiCd batteries are well developed for consumer applications but also used for large-scale applications. Compared to lead-acid batteries, they have lower cell voltage, as shown in Equation 2,

$$\mathrm{Cd} + 2\,\mathrm{NiOOH} + 2\,\mathrm{H_2O} \Leftrightarrow \mathrm{Cd(OH)_2} + 2\,\mathrm{Ni(OH)_2} \qquad E^0 = 1.29\ \mathrm{V}, \tag{2.}$$

but higher energy density and longer cycle life. However, other batteries are replacing NiCd batteries in all markets owing to their substantial negative temperature coefficient that limits charging, voltage depression (memory effect), high cost, and environmental concerns (3). Key manufacturers of NiCd batteries are Storage Battery Systems and Saft Batteries (**http://www.saftbatteries.com**). The latter installed the biggest NiCd battery for a stationary application (a spinning reserve and power stabilization system) in Alaska (a 40-MW unit built with 13,760 cells).

Nickel metal-hydride batteries. Although they have been on the market for more than 20 years as portable and then traction batteries, secondary nickel-metal hydride (NiMH) batteries have only recently been considered for stationary applications such as UPS and telecom (23). NiMH batteries have higher specific energy and better heat tolerance (up to 70°C), which are important for telecom applications, plus they do not exhibit the memory effect that NiCd batteries do. Ovonic Battery Company (**http://www.energyconversiondevices.com**) (23) advertises a 560-kW battery for UPS, telecom, and solar applications with one-third of the lead-acid battery footprint.

The cell chemistry of NiMH batteries is described by Equation 3,

$$MH + NiOOH \Leftrightarrow M + Ni(OH)_2 \qquad E^0 = 1.35\ V. \qquad 3.$$

M in this equation is an intermetallic compound of composition AB_5, where A is a combination of La, Ce, Pr, and Nd, and B is a combination of Ni, Co, Mn, Al, or AB_2, where A is a combination of Ti, V, and Zr, and B is a combination of Ni, Co, Cr, Mn, Al, and Sn. The partial substitution of Ni by Al or Mn in the $La(Ni,M)_5$ phase yields increased discharge capacity, and addition of Co greatly improves the cycle life (24). Optimization of alloy composition and an increase in the structural disorder allowed increased specific energy and stability to the alkaline environment (25). It is necessary to balance the effects of different additives; for example, addition of Fe to AB_2 compositions decreases specific power but increases cycle life, whereas addition of Sn decreases storage capacity but reduces the cost (26).

The electrolyte is usually aqueous 30% potassium hydroxide with added LiOH to improve the cathode charging efficiency. Gelation of the electrolyte with polyethylene oxide (PEO) improves reversibility and electric efficiency up to 80% (27).

Sodium-sulfur batteries. Sodium-sulfur (NAS) batteries are considered one of the most promising candidates for stationary EES. They are used for load leveling and peak shaving as well as spinning and standby reserves. They are also proposed for smoothing the output from intermittent renewable energy sources. The battery consists of a molten sulfur cathode and molten sodium anode separated by Na^+-conducting ceramics, usually β''-alumina (β''-Al_2O_3). During discharge sodium is oxidized and sulfur is reduced to form sodium polysulfides Na_2S_x ($x = 3$–5) in the cathode compartment, as shown in Equation 4:

$$2Na + x\,S \Leftrightarrow Na_2S_x \qquad E^0 = 2.07 - 1.78\ V. \qquad 4.$$

At the battery working temperature (300–350°C) all electroactive materials are in liquid form. To compensate for the low conductivity of sodium polysulfides in sulfur, carbon felt is used as a current collector, thus increasing the battery cost. Sodium is stored inside a tubular container made of the primary solid electrolyte that is surrounded by the cathode (the central sodium geometry). The NAS battery has zero self-discharge and high electrical efficiency. Due to high working temperatures, the heat losses may be substantial enough during standby or floating charge (ohmic heating when the battery is charged or discharged usually compensates for the heat losses) to be practically equivalent to a self-discharge. It should be noted that the reaction between molten sodium and sulfur is highly exothermic, thus increasing the fire hazard, and, in the absence of electronics to detect and shunt around failed cells, the broken cell turns off the whole string because sulfur and sodium sulfides are insulators.

The current chemistry-related research work on the NAS battery mainly targets corrosion-resistant sealing and containment materials and a low-resistance β''-alumina separator with a dense and fine-grained microstructure (28). Addition of yttria-stabilized zirconia (YSZ) or ceria (cerium dioxide) using a novel vapor phase process that involves exposure of sintered mixture of α-alumina and YSZ to soda vapor at ~1,450°C to convert α-alumina into β''-alumina yields fine-grain ceramics (29, 30). The use of ζ-aluminates, $M_2O \cdot 5Al_2O_3$ ($M = Na, Li$), as precursors has allowed the production of ceramic tubes with low resistivity (31).

A novel room-temperature NAS battery with a solid Na anode, solid sulfur or metal sulfide cathode, liquid glyme or carbonate electrolyte, and a Celgard separator has been proposed

(32, 33). The initial discharge capacity (489 mAh/g sulfur) was close to that of the high-temperature NAS battery but rapidly decreased with cycling (32).

NGK Insulators Ltd. of Japan (**http://www.ngk.co.jp**) is currently the only supplier of NAS batteries. The size of NAS installations coupled with renewable sources varies from 1 to 65 MW (6 to 150 MWh). Recently, Pacific Gas & Electric Company announced it would install a 4-MW NAS system with a 28-MWh storage capacity, which would be the biggest battery-based EES in California (**http://www.energy.ca.gov**).

Emerging Technologies

Some battery technologies, such as Li-ion, are well developed for the consumer market but only recently began to penetrate into the stationary EES market. Experimental data in the field are limited, and therefore these technologies are considered as emerging ones.

Lithium-ion batteries. Lithium-ion batteries use lithium intercalation in both the positive (lithium metal oxides) and negative (usually graphitic carbon) materials in an organic electrolyte, as shown in Equation 5:

$$Li_xC + Li_{1-x}MO_2 \Leftrightarrow LiMO_2 + C \qquad E^0 = 3.3 - 4.2\ V. \qquad 5.$$

Lithiated carbon is protected from reaction with the electrolyte by a solid-electrolyte interphase (SEI) (34). The advantages of Li-ion batteries include high cell voltage and energy density, low self-discharge, and excellent rate capabilities. Major shortcomings are high cost, low temperature tolerance, and the need for protective circuitry to prevent cell degradation and thermal runaway. Lithium polymer batteries use the same chemistry but a solid polymer as the electrolyte; they provide improved safety and more flexible cell design but at the expense of increased cost and decreased scalability.

Li-ion technology (35) is currently a favorite for consumer and mobile applications and received a boost with the development of plug-in and electric cars. Major breakthroughs in this technology were the use of $LiFePO_4$ as cathode material (36), especially in the doped nanosized form (37); a safer anode material, $Li_4Ti_5O_{12}$ (38); and advanced electrolytes (39). Recent advances in this technology have translated into increasing numbers of EES installations (40). For example, A123 Systems (**http://www.a123systems.com**) has built a Li-ion grid storage battery for AES Energy Storage (12-MW installation in Chile and 20 MW in New York for frequency regulation) and for Southern California Edison. Altair Nanotechnologies (**http://www.altairnano.com**), working with AES Energy Storage, has deployed a 1-MW, 250-kWh Li-ion battery system using lithium titanate capable of full charging and discharging in 15 minutes (4C rate) for grid regulation. Valence Technology (**http://www.valence.com**) will install EES based on batteries with a $LiFeMgPO_4$ cathode for the first smart grid solar-powered residential development in Texas. Saft Batteries has developed large Li-ion batteries with maximum power 150 W kg^{-1} at two hour (C/2) discharge rate, maximum energy 65 Wh kg^{-1} at 15 minutes discharge (4C rate), low self-discharge (less than 5% per year), and a faradic efficiency close to 100% for telecom and stationary applications. Ener1 Battery Company (**http://www.ener1.com**) is already building five 1-MW Li-ion battery grid storage trailers for Oregon's Portland General Electric. Similarly, Sony and Lithium Technology Corporation have announced $LiFePO_4$-based packs for integration with household photovoltaic systems (**http://www.gaia-akku.com**).

Sodium metal chloride batteries. The sodium metal chloride battery was invented more than 25 years ago within the ZEolite Battery Research Africa (ZEBRA) project by Coetzer's group in

South Africa (41). The chemistry is based on the electrochemical reaction of molten sodium in the anode with transition metal chloride in the cathode (discharge) and the reverse reaction of the transition metal with NaCl (charge) (Equation 6):

$$MCl_2 + 2\,Na \Leftrightarrow M + 2\,NaCl \qquad E^0 = 2.58\ V(M = Ni), \quad 2.35\ V(M = Fe). \qquad 6.$$

As in the case of a NAS battery, the anode and cathode are separated by the Na^+-conductive β''-Al_2O_3 ceramic membrane. Ionic conductivity in the cathode is provided by a secondary electrolyte, molten sodium aluminum tetrachloride ($NaAlCl_4$). Many transition metals (42, 43, 30) have been tested as active cathode materials; nickel and iron (Equation 6) are the most practical. Current commercial ZEBRA batteries contain a mixture of nickel and iron, which is added to improve the battery power (44, 45). The cathode contains an excess of nickel powder, which serves as an extended current collector and reduces cell resistance. The downside of this approach is low utilization (25–30% or even lower in NiFe cells) of expensive nickel.

This simple chemistry, however, cannot provide long cycle life. Morphology changes have been proposed as the mechanism of capacity loss during cycling (46). Addition of elemental sulfur (1–5%) to the dense cathodes yielded significant improvement in the capacity retention (46). The reduction of S, which was found in the cycled cathode by the X-ray diffraction in the form of Ni_3S_2, prevented grain growth of the Ni particles in the cathode and promoted formation of a modified high–surface area, active metallic phase that was stable for hundreds of cycles (47). The β''-alumina electrolyte tube was stable in contact with the S-doped Ni cathode electrolyte for more than 2,000 cycles. Combination of sulfur with NaI and NaBr additives reduced the area-specific impedance of the nickel chloride electrode (48).

Recent research on sodium metal chloride batteries has focused on improvement of the cathode composition to increase energy and power. Optimization of the concentration of FeS (instead of elemental sulfur) and NaI cathode additives yielded an energy increase from 94 Wh kg^{-1} to 120 Wh kg^{-1} in commercial batteries (45). It was suggested that NaI generates nickel iodide that serves as a charge transfer mediator (49).

Sodium metal chloride batteries are assembled in the discharged state, with the cathode consisting of nickel and iron, NaCl, and small amounts of additives to improve performance, and then impregnated under vacuum with molten $NaAlCl_4$. In contrast to NAS batteries, the preferred design for ZEBRA batteries has a central cathode geometry. Instead of round β''-alumina tubes, cruciform (cloverleaf)-shaped tubes are used to increase the battery power by increasing the surface area of the secondary electrolyte and the reaction front (50, 51). EaglePicher (**http://www.eaglepicher.com**), in partnership with the Pacific Northwest National Laboratory and funded by Advanced Research Projects Agency–Energy, is developing a battery with a planar configuration of thinner electrodes that may provide higher power. Sodium is generated in the anode compartment during the first charge. This feature makes sodium metal chloride batteries safer to manufacture than NAS batteries because no elemental sodium is involved in cell assembly. In addition, the most common failure mode of molten sodium batteries—a broken β''-alumina separator tube—in this case yields a relatively mildly exothermic reaction between Na and the electrolyte (Equation 7):

$$NaAlCl_4 + 3\,Na \rightarrow Al + 4\,NaCl. \qquad 7.$$

The aluminum metal generated in this reaction shorts the cell, which keeps the whole string operational, as opposed to what occurs in NAS batteries (51). In addition, sodium metal chloride batteries are much more tolerant to freeze-thaw cycles than NAS batteries owing to smaller differences in thermal expansion coefficients between the ceramic separator and other battery components.

The cells are packaged in a double-walled vacuum-insulated metal box equipped with an air cooler and an ohmic heater controlled by the battery management system (BMS) to keep the cell temperature constant at approximately 300°C (45, 52). As in the case of NAS batteries, the heat losses should be compensated and can be considered as equivalent to self-discharge.

ZEBRA batteries have been developed primarily for mobile applications. MES-DEA of Switzerland (now FZ Sonick SA; **http://www.cebi.com/cebi**) currently produces batteries for mobile applications (e.g., electric buses) with a production capacity of 90 MWh annually. Additionally, systems for vehicle-to-grid (V2G), telecom, and distributed energy generation coupled with renewable sources applications are planned (53, 45). Recently, GE (**http://www.geenergystorage.com**) announced plans to build an improved sodium metal chloride Durathon^{TM} battery plant with the capability of generating 900 MWh of energy per year to serve mainly UPS, telecom, utility, and heavy-duty transportation applications. Xylene Power Ltd. (**http://www.xylenepower.com**) is developing a sodium-sulfur-nickel chloride (Na-S-$NiCl_2$) electrochemical cell that the company claims will combine the best properties of NAS and sodium–nickel chloride batteries. This 18-kWh battery is reported to have a lifetime of approximately 2,000 cycles and a specific energy density of approximately 100 Wh kg^{-1} (812 Wh kg^{-1} theory).

New Chemistries

To improve the safety of Li-ion batteries, batteries with aqueous electrolytes ($LiNO_3$, Li_2SO_4) have been proposed (54). The cell voltage is limited by water, and the cycle life of such batteries is short. However, it was recently shown that exclusion of oxygen and pH adjustment in the $LiTi_2(PO_4)_3/Li_2SO_4/LiFePO_4$ cell allowed good capacity retention (10% capacity loss over 1,000 cycles) (55).

A major research direction aims to replace materials with limited capacity, in particular carbon as an anode material and metal oxides as cathode materials, with potentially much higher capacity materials: lithium metal and transition metal fluorides, respectively. Badway et al. (56) provided the first practical demonstration that FeF_3 as a nanocomposite with carbon may be reversibly cycled at 235 mAh g^{-1} to FeF_2 and at 600 mAh g^{-1} (770 mAh g^{-1} theory) to metal iron, which is much higher than the capacity of $LiCoO_2$ (150 mAh g^{-1}). Other promising cathode materials are TiF_3, VF_3, CuF_2, BiF_3, CoF_2, and NiF_2 (57, 58). Metal fluorides (as well as sulfides and nitrides) that transfer two or three electrons overcome the one-electron limitation of the complex metal oxides. Unfortunately, these materials are insulators and react with lithium to form new phases (LiF and metal or mixed phases). In contrast, transition metal oxides that form intercalation compounds have essentially the same crystal structures as their parent mixed oxides. Suggestions to make Li transport reversible include decreasing the particle size and optimizing the cathode composite (which includes a conductive additive) microstructure as well as using material doping.

When used as an anode material, lithium metal has approximately 10 times more capacity than the lithium-carbon intercalated materials currently used in Li-ion batteries. Lithium reacts with oxygen (Equations 8 and 9) and sulfur (Equation 10) as follows:

$$\mathrm{Li} + {}^{1}\!/\!_{4}\mathrm{O_2} + {}^{1}\!/\!_{2}\mathrm{H_2O} \Leftrightarrow \mathrm{LiOH}(\text{in aqueous electrolyte}) \qquad E^0 = 3.44\ \mathrm{V}, \tag{8}$$

$$2\,\mathrm{Li} + \mathrm{O_2} \Leftrightarrow \mathrm{Li_2O_2}(\text{in non-aqueous electrolyte}) \qquad E^0 = 2.96\ \mathrm{V}, \tag{9}$$

$$2\,\mathrm{Li} + \mathrm{S} \Leftrightarrow \mathrm{Li_2S} \qquad E^0 = 2.2\ \mathrm{V}. \tag{10}$$

Such couples have the highest theoretical energy density among rechargeable batteries (3,860, 3,500, and 2,460 Wh kg^{-1}, respectively). However, poor Li reversibility that requires a large excess of the metal (three- to fourfold) as well as safety issues (dendrite formation and the inherent thermodynamic instability of Li metal in organic solvents) limits its use in batteries. Li-air batteries also suffer from poor reversibility of oxygen reduction (59). Nevertheless, the potential increase in energy density, especially in combination with energy-dense sulfur and oxygen cathodes, has stimulated further research on protection and cycling reversibility of lithium metal in such batteries with different cathodes.

In the case of aqueous electrolyte [usually basic but an acidic electrolyte also could be used (60)], reaction products are soluble and do not block the membrane. Solid-state electrolytes are considered promising for lithium metal batteries to provide safety and long cycle life. A protective layer for Li called LISICON [$LiM_2(PO_4)_3$] has been patented (61) and used by PolyPlus (**http://www.polyplus.com**) and SION Power (**http://www.sionpower.com**) in rechargeable Li-air and Li-S batteries. An all-solid-state Li-S battery with a glass ceramic lithium thiophosphate electrolyte also exhibited excellent capacity retention (62). Furthermore, Seeo (**http://www.seeo.com**) is developing an all-solid lithium metal battery with $LiFePO_4$ or sulfur cathodes (63) and a novel PEO-based solid polymer electrolyte invented at Lawrence Berkeley National Laboratory (64, 65).

The Japan National Institute of Advanced Industrial Science and Technology (AIST) (**http://www.aist.go.jp**) is developing a rechargeable lithium-air battery that uses two types of electrolytes. An organic electrolyte conducts Li^+ ions from/to metal lithium in the anode, which is separated from the cathode by a solid ionic conductor (e.g., LISICON). LiOH formed in the cathode by oxygen reduction is soluble in aqueous alkaline electrolyte. Inexpensive Mn_3O_4 on carbon is used as the oxygen reduction catalyst in alkaline media (66, 67). A separate electrode in the cathode is used for battery charging. An all-solid Li-air battery with a layered membrane made from glass-ceramic and polymer-ceramic materials and a solid-state composite air cathode demonstrated a potential energy density of 1,000 Wh kg^{-1} (68).

A Li foil anode protected by a solid-state Li^+-conducting membrane in combination with an organic electrolyte was used for a novel Ni-Li battery with the common $Ni(OH)_2$ cathode in an alkaline electrolyte (69). This battery has high cell voltage (3.49 V) and energy density (935 Wh kg^{-1} theoretical and >400 Wh kg^{-1} projected practical) (69).

The reversibility of a Li-S battery is much better than that of a Li-air battery. The chemistry of a Li-S battery is more complex than that described by Equation 10 and includes equilibria between several lithium polysulfides with different solubility and redox potentials (70–74). Polysulfides react with lithium to cause substantial self-discharge, which may be reduced by selection of mixed solvents for the electrolyte (75). A practical energy density of 350 Wh kg^{-1} for this battery has been demonstrated (76). In addition, silicon nanowires have been used as a low-expansion matrix for lithium electroplating in a lithium-sulfur battery. A battery with a Li_2S-impregnated mesoporous carbon cathode and a Si nanowire anode has low resistance and high theoretical energy density (1,550 Wh kg^{-1}) but, unfortunately, poor capacity retention (77).

To address the problem of lithium instability in organic electrolytes, Arizona State University, in collaboration with Fluidic Energy, Inc. (**http://fluidicenergy.com/**), is developing a new class of metal-air batteries using ionic liquids as electrolytes. It was claimed that these batteries would have lower cost and a target energy density more than six times higher than that of available Li-ion batteries (78). A battery with a molten alkali bis(trifluoromethylsulfonyl) amide mixture as an electrolyte with a Li metal anode and $LiFePO_4$ cathode at 100–180°C demonstrated good capacity retention (79).

Cairns et al. (80) introduced the concept of an all-liquid membraneless battery in which reaction products are dissolved in a fused salt electrolyte. In such high-temperature battery liquid, lithium was used as the anode, a lithium halide eutectic as the electrolyte, and bismuth, selenium, tellurium

(80), or P_4S_{10} (81) as the cathode. Sadoway et al. (82) have introduced a new all-liquid battery for stationary applications based on Equation 11,

$$3\,\mathrm{Mg} + 2\,\mathrm{Sb} \Leftrightarrow \mathrm{Mg_3Sb_2} \qquad E^0 = 0.42\ \mathrm{V}, \tag{11.}$$

and consists of three layers of liquids—magnesium, sodium sulfide, and antimony—that are naturally separated by gravity owing to significant density differences. The battery works at 700°C, and the reaction product, Mg_3Sb_2, is dissolved in the sulfide electrolyte during the battery discharge. The simple design, absence of a separator between anode and cathode, and high current density make this battery attractive for large-scale applications. However, low cell voltage and extremely high temperature of operations (which means expensive materials of construction and heat losses) are clear disadvantages.

FLOW BATTERIES

The redox flow battery concept has been around since the 1970s but is still a less developed technology compared with lead-acid and NiCd secondary batteries (4). Only two types of flow batteries (all-vanadium and polysulfide-bromine) have reached commercialization on a large scale. A flow battery consists of two usually aqueous electrolytes that contain two redox couples and are pumped through an electrochemical cell in which chemical energy is converted to electricity. The two electrolytes are stored in separate tanks and separated in the electrochemical cell by an ion exchange (cation or anion) membrane (**Figure 1**). Ideally, the membrane should be impermeable to redox-active species but allow the transport of cations (usually protons or Na^+) or anions, and sometimes water, to maintain electroneutrality and electrolyte balance. There are seven redox couples suitable for flow batteries (V/V, S/Br_2, Zn/Br_2, V/Br_2, Fe/Cr, Ce/Zn, and Pb/Pb) that are in different stages of pilot testing (4). Two other redox couples Zn/Cl_2 and H_2/Br_2 are at the laboratory testing stage.

The most important feature of redox flow batteries is the potential to separate the energy capacity and the power. The battery energy capacity is determined by the size of the electrolyte tanks, whereas the battery power is defined by the size of the electrochemical cell. This allows for a flexible layout, which is attractive for stationary applications. Additional advantages of redox flow batteries include the ability to fully charge and discharge without damaging the cell, the long

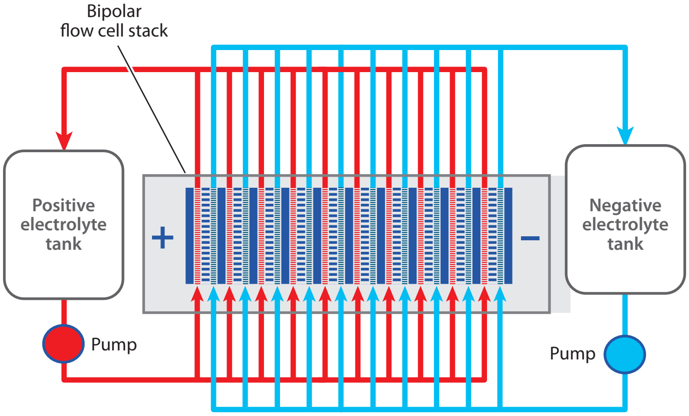

Figure 1

Redox flow battery concept.

life of the electrolytes (basically, the battery lifetime is defined by the lifetime of the ion-selective membrane), flexible operation, modular design, and moderate cost. For instance, the projected life of vanadium redox batteries is 8 years, after which the membrane could be replaced to extend the lifetime (83). In addition, thermal management of flow batteries is easier than that of other types of batteries owing to the flow of liquid electrolytes. The main drawbacks of flow batteries are the low energy density, which is limited by solubility of redox-active species; the cross-contamination; and the longevity of ion-selective membranes. Because a stack of electrochemical cells with bipolar electrodes is typically used, the shunt current may substantially decrease the battery efficiency. This negative effect could be reduced by increasing the manifold length of the cell ports, but this increases energy losses for pumping, so trade-offs should be made. Furthermore, the plumbing, pumping, and connections in flow batteries are complex and prone to leakage, which increases maintenance cost.

Mature Technologies

Several redox flow battery technologies have been tested in the field long enough to collect data on their reliability and efficiency. As a result, the initial concept of storing energy in big electrolyte tanks has been changed to a modular design with a much smaller scale for a single unit.

Vanadium redox flow battery. The concept of vanadium-vanadium, also known as the all-vanadium redox battery (VRB), was suggested in 1984 at the University of New South Wales, Australia (83). The battery uses the V^{V}/V^{IV} and V^{III}/V^{II} redox couples in sulfuric acid as the positive and negative half-cell electrolytes, respectively (84). The cell chemistry is represented by the total Equation 12:

$$VO_2^+ + 2\,H^+ + V^{2+} \Leftrightarrow VO^{2+} + H_2O + V^{3+} \qquad E^0 = 1.26\text{ V}. \tag{12}$$

The initial electrolyte is prepared as a mixture of 1 M V^{III} and V^{IV} by chemical reduction or electrolytic dissolution of V_2O_5 in H_2SO_4. To balance electroneutrality, protons should move between cathode and anode via a proton exchange membrane.

The VRB can be recharged both electrochemically and mechanically by replacing spent solutions with fresh ones. In the discharged state, the positive and negative electrolytes are essentially the same, which prevents migration of ions between anolyte and catholyte. Ion migration in the charged state causes a self-discharge that may reach 3% per day. However, this is not fatal for the battery because it can be recharged back to the full capacity. Turning off the pumps effectively reduced the self-discharge. Additionally, much lower self-discharge was found for the proton exchange membranes modified with polyethyleneimine (85), polypyrrole (86), or alternating layers of a polycation and polyanion (87). A novel fluoropolymer-based amphoteric ion exchange membrane and sulfonated poly(fluorenyl ether ketone) membrane exhibited lower vanadium crossover and higher efficiency than Nafion® membranes (88, 89). Hybrid-structure membranes based on a sulfonated poly(fluorenyl ether ketone) ionomer with embedded silica demonstrated enhanced proton selectivity in a VRB (90). Furthermore, addition of a conductive material to the electrolyte decreased the cell resistance and increased power (91). According to a recent study, the net energy storage efficiency is higher and the environmental impact is substantially lower for the vanadium-vanadium battery than for the lead-acid battery (92).

The major suppliers of vanadium redox batteries are VRB Power Systems, Inc. (now Prudent Energy, China; **http://www.pdenergy.com**) and Sumitomo Electric Industries (SEI). VRB Power built a 250-kW, 2-MWh prototype system for PacifiCorp in Utah and several systems from 100 kW to 4 MW for peak shaving, UPS, and renewables in Japan. SEI installed a 450-kW/1-MWh, 2-h VRB load-leveling demonstration system and a 3-MW UPS system in Japan (93). Ashlawn Energy will install a 1 MW/8 MWh VRB in Ohio under the DOE's Smart Grid program using VFuel Pty Ltd. (**http://www.vfuel.com.au**) technology. In addition, Cellennium Co. (Thailand; **http://www.vanadiumbattery.com**) is developing a 50-kW VRB made of horizontal bipolar flow cells arranged in a vertical pile that greatly reduces shunt current.

Polysulfide-bromine flow battery. The chemistry of the polysulfide-bromine (PSB) flow battery is based on the redox reaction of sodium polysufides and the couple $Br^-/Br_3{}^-$, as shown in Equation 13:

$$2\,Na_2S_2 + NaBr_3 \Leftrightarrow Na_2S_4 + 3\,NaBr \qquad E^0 = 1.36\ V \qquad 13.$$

(94). The open circuit voltage depends on the concentration of active species and varies from 1.7 to 1.5 V. Ideally, only Na^+ cations pass through a cation-selective membrane, e.g., Nafion®. Due to the higher solubility of electroactive species, PSB has a higher energy density (30 W h kg^{-1}) than other flow batteries. In one study, replacing a carbon current collector in the negative electrode with nickel foam increased the efficiency of a PSB up to 77% (95). One of the challenges for PSB batteries is maintaining the water balance to avoid dilution of one of the electrolytes. The use of a buffer chamber could alleviate this problem (96). Other challenges are cross-contamination, deposition of insoluble sulfur species on the membrane, and gas (H_2S, Br_2) evolution.

Regenesys successfully tested a 1-MW prototype and had ambitious plans to build 12-MW, 120-MWh plants in Little Barford, UK, and in Columbus, Mississippi. However, a new owner, German utility company RWE, canceled these projects in 2003. The PSB technology has been acquired by VRB Power (now Prudent Energy).

Emerging Technologies

Redox flow batteries reviewed here vary from rather old to recently introduced. However, they all are built at a relatively small scale and have not had enough time in the field to be considered mature.

Zinc-bromine and zinc-chlorine flow batteries. The zinc-bromine flow battery (ZBB) consists of a zinc anode and a bromine cathode separated by a microporous separator. An aqueous solution of zinc bromide, which is the battery discharge product, is circulated through the two compartments of the cell from two separate tanks. Bromine is stored adsorbed on porous media or in the form of a complex with quaternary ammonium cations that is in equilibrium with an aqueous bromine-containing phase (97). The reaction chemistry is:

$$Zn + Br_3^- \Leftrightarrow ZnBr_2 + Br^- \qquad E^0 = 1.85\ V. \qquad 14.$$

The battery uses an inexpensive porous diaphragm to separate anolyte and catholyte. Because the electrode kinetics of a Zn/Zn^{2+} couple is much faster than that of a Br_2/Br^- couple, high–surface area carbon electrodes are used on the cathode side.

The major drawbacks of ZBB are the high cost of electrodes, zinc dendrite formation during charge, low energy efficiency, and poor cycle life (4). Nevertheless, due to its high energy density (75–85 Wh kg^{-1}), insignificant electrode polarization, and low cost, ZBB has been considered for load leveling applications.

ZBB Energy Corp. (**http://www.zbbenergy.com**) sells ZESS POWR™ modules with up to 250 kW power and up to 400 kWh storage capacity as well as systems built from up to 20 modules with 8,000 kWh storage capacity total. Recently ZBB Energy Corp. and SunPower announced the pairing of a 500-kWh system with photovoltaic solar for a commercial building application. Premium Power (**http://www.premiumpower.com**) builds the modular PowerBlock® 150 and TransFlow 2000 utility-grade energy management systems, which use the zinc-bromide Zinc-Flow® technology and provides 100 kW or 500 kW of uninterrupted power and 150 kWh or 2.8 MWh of energy storage capacity, respectively. RedFlow (**http://www.redflow.com.au**) markets a modular 200-kW/400-kWh zinc-bromine flow battery mostly for telecom and solar applications. Primus Power (**http://www.primuspower.com**) participates in a project to commercialize a 25-MW/75-MWh system in California as part of DOE's Smart Grid Demonstration Program.

The zinc-chlorine flow battery has similar features and chemistry (Equation 15):

$$\mathrm{Zn} + \mathrm{Cl_2} \Leftrightarrow \mathrm{ZnCl_2} \qquad E^0 = 2.02\ \mathrm{V}. \qquad 15.$$

It uses liquefied chlorine and a NaCl electrolyte and has higher open circuit voltage than the bromine analog (98).

Cerium-zinc flow battery. The recently suggested cerium-zinc flow battery forms a solid during charge (Equation 16),

$$2\,\mathrm{Ce(CH_3SO_3)_4} + \mathrm{Zn} \Leftrightarrow 2\,\mathrm{Ce(CH_3SO_3)_3} + \mathrm{Zn(CH_3SO_3)_2} \qquad E^0 = 2.48\ \mathrm{V}, \qquad 16.$$

similar to the zinc-bromine battery (99). Both anode and cathode compartments include methane sulfonic acid (MSA) as an electrolyte, so both cerium and zinc are present in solution as salts with the MSA anion. Only protons pass through the proton exchange membrane (e.g., Nafion®) during charge and discharge, and their concentration is high enough to dissolve dendrites formed from the electrodes. To prevent hydrogen evolution, the hydrogen overpotential was increased by addition of small amounts of indium or tin (99). Remarkably, the battery is not sensitive to cross-contamination, which may even be beneficial (100).

Plurion (**http://www.plurionsystems.com**) is developing a 250-kW modular cerium-zinc system for UPS and renewables made of four 65-kW batteries.

Iron-chromium flow battery. The iron-chromium flow battery was invented by Thaller (101) and has the chemistry

$$\mathrm{Cr^{2+}} + \mathrm{Fe^{3+}} \Leftrightarrow \mathrm{Cr^{3+}} + \mathrm{Fe^{2+}} \qquad E^0 = 1.18\ \mathrm{V}. \qquad 17.$$

The cell was later improved by NASA in the 1980s (102, 103) and at the University of Alicante in the 1990s (104–106). Two one-electron redox couples ($\mathrm{Fe^{II}/Fe^{III}}$ and $\mathrm{Cr^{II}/Cr^{III}}$) in hydrochloric acid are used as the positive and negative reactants. The ion-selective membrane should allow only protons and chloride anions to pass but in reality cannot prevent cross-contamination.

The open circuit voltage changes with the charge state because of the dominance of different hydrated complexes of $\mathrm{Cr^{III}}$ at different stages (107). The slow chromium redox kinetics called for the development of redox catalysts such as bismuth or bismuth-lead on carbon (108). Alternatively, addition of ethylenediaminetetraacetic acid (EDTA) to the chromium electrolyte stabilizes $\mathrm{Cr^{V}}$, which makes an all-chromium battery possible, but the kinetics of the anodic reaction is slow (109).

Deeya Energy (**http://www.deeyaenergy.com**) commercializes the iron-chromium flow battery. The product, Energy Storage Platform 24 K™, is a module capable of delivering 24 kWh day^{-1}. The company claims that due to improved performance, cost, and life (10,000 cycles) the system cost is approximately three times less expensive than lead-acid batteries.

New Chemistries

The high cost of vanadium redox flow batteries has stimulated research on a vanadium-bromine battery, which uses vanadium only in the negative half-cell and a bromine/bromide couple in the positive half-cell of the battery, as shown in Equation 18:

$$2\,V^{2+} + Br_2 \Leftrightarrow 2\,V^{3+} + 2\,Br^- \qquad E^0 = 1.32\ V \qquad 18.$$

(110). This approach reduces the battery cost by approximately 40% and almost doubles the energy density (up to 50 Wh kg^{-1}) owing to the higher solubility of bromide. Another possible couple is chromium-bromine, which has a theoretical energy density of 57 Wh kg^{-1} (111). A cerium-vanadium couple demonstrated a higher open circuit voltage of 1.87 V with a coulombic efficiency of 87% (112).

Pletcher et al. (113–120) recently proposed a new soluble lead-acid flow battery. The electrode reactions are the same as in the classic lead-acid battery (Equation 1) and have been studied in different electrolytes (4), but the high solubility of Pb^{II} in methanesulfonic acid allows it to be carried in a flowing solution. Because both charge products, Pb and PbO_2, are insoluble, and the soluble discharge product $Pb(MSA)_2$ is common for both electrodes, the cell can be run in the undivided mode. The voltage during discharge is approximately 1.55 V, and the energy efficiency is 65% (113). It is possible to deposit thick layers of PbO_2, but its reduction is difficult. Additives such as sodium lignin sulfonate give uniform deposits without dendrites (116). However, the current density of this battery is limited because of the high overpotential for the PbO_2 deposition and oxygen evolution (117).

Another undivided flow battery employing porous flow through electrodes and $Ru(acac)_3$ (acac = acetylacetonate) and $Fe(bpy)_3(ClO_4)_2$ (bpy = bipyridyl) in acetonitrile has been suggested (90), but low concentrations of redox active species make it impractical despite the cell design simplicity.

Uranium β-diketone complexes in polar aprotic solvents were proposed as excellent active materials in an all-uranium redox flow battery with U^{VI}/U^{V} solution as the positive electrolyte and U^{IV}/U^{III} solution as the negative electrolyte (121). The concentrations of uranium solutions may be as high as 0.8 M and the open circuit cell voltage 1 V for acetylacetone and higher for ligands with greater basicity (121). Tetraketones form even stronger complexes with uranium and are better suited as active materials (122).

Several electroactive couples for redox flow batteries have been suggested, one of which is a Mn^{III}/Mn^{II} redox couple for the cathodic electroactive material (123). Complexes of iron with triethanolamine, EDTA, or citrate in combination with bromine were used in a flow battery and exhibited an open circuit voltage of nearly 2.0 V at full charge and an energy efficiency of approximately 70% (124, 125). Complexing cerium with diethylenetriaminepentaacetate improves the electrode kinetics of the Ce^{IV}/Ce^{III} couple for the positive electrolyte (126).

In another example, a novel hybrid single-flow Zn/NiOOH battery demonstrated a high energy efficiency of 86% over 1,000 cycles. A highly concentrated ZnO solution in aqueous KOH was used as the electrolyte, and the positive electrode was the nickel oxide used for secondary alkaline batteries. At battery charging, $Ni(OH)_2$ is oxidized to NiOOH and zincate ions are reduced to zinc, which is electroplated onto the anode; no membrane is required (127). Another new single-flow acid battery, a Cu-PbO_2 battery with H_2SO_4-$CuSO_4$ electrolyte, has been proposed (128). Only one electrolyte is pumped through the battery during charge and discharge; no membrane is needed. Preliminary tests showed energy efficiency of 83% during 450 cycles at a discharge voltage of 1.29 V (128).

REGENERATIVE FUEL CELLS

A regenerative fuel cell (RFC) can operate both as a fuel cell (discharge mode) and as an electrolyzer (charge mode). Only hydrogen proton exchange membrane (PEM) fuel cells can work in both directions. During charge the RFC generates hydrogen and oxygen that are stored in storage tanks, and during discharge it electrochemically oxidizes hydrogen to generate power (129). The electrolyzer and the fuel cell may be separate units or integrated in a single stack (unitized RFC). The theoretical specific energy of the hydrogen/oxygen couple is 16,470 Wh kg^{-1}. Current RFC systems have demonstrated an overall specific energy density from 400 to 1,000 Wh kg^{-1}, which is still several times higher than that of any secondary battery. Therefore, regenerative H_2/O_2 fuel cells have potentially the highest specific energy densities among known energy storage systems (130).

GE (131) proposed a rechargeable fuel cell combining a metal hydride electrode with the air electrode. Hydrogen produced by water electrolysis is stored in the anode during charging and then consumed during discharge to generate power. The theoretical specific energy density of a rechargeable fuel cell with an anode containing $LaNi_5H_6$ or MgH_2 can reach 458 and 1,900 Wh kg^{-1}, respectively. The main disadvantages of such systems are electrode deterioration during the oxygen evolution reaction and alkaline electrolyte poisoning by CO_2. To prevent this, a second cathode (132) and a scrubber (133) were added to the system, which reduced the overall energy density.

Adding gas diffusion electrodes to a common NiMH battery and supplying hydrogen to the anode and oxygen to the cathode yields a combination of a fuel cell and a secondary battery (134). Small amounts of MnO_2 in the $Ni(OH)_2$ cathode convert it into the catalytically active oxygen electrode of the fuel cell. The system can be used as a secondary battery if hydrogen and oxygen are not supplied.

Another way to avoid the oxygen reduction problem is to replace O_2 with chlorine or bromine. The H_2/Br_2 couple has a lower cell voltage than the H_2/O_2 couple (0.555 V versus 1.229 V) but much higher efficiency in the fuel cell mode (135, 136). EnStorage (Israel; **http://www.enstorageinc.com**) is developing EES systems based on regenerative H_2/Br_2 fuel cells having significantly higher efficiency (~90%) than H_2/O_2 fuel cells (~40%) (137). Recently, Lawrence Berkeley National Laboratory (**http://www.lbl.gov**) announced plans to develop a hydrogen-bromine system for grid applications in cooperation with DuPont, Bosch, 3M, and Proton Energy.

To overcome the problems of slow kinetics and high overpotential for the oxygen reduction reaction (ORR), several attempts to use hydrogen peroxide instead of oxygen have been made. A novel, though more complicated, pathway for EES using a combination of an electrolyzer and a fuel cell based on the two-electron reduction of oxygen has been suggested (138). Energy is stored in the form of aqueous H_2O_2 produced by electrolysis and is released by electrolytic decomposition of H_2O_2 to H_2 and O_2, which are directed to a PEM fuel cell. The energy density of aqueous H_2O_2 in this case is 136 Wh kg^{-1}, which is higher than that of common flow batteries, but the overall efficiency is lower (35%) (138).

Hydrogen storage and transportation is energy inefficient and expensive. Therefore, several approaches have been used to avoid handling of hazardous hydrogen gas. A new $NaBH_4/H_2O_2$ all-liquid fuel cell with an OH^--ion-conducting anion exchange membrane has a much higher cell voltage, as seen in Equation 19,

$$NaBH_4 + 4\,H_2O_2 \Leftrightarrow NaBO_2 + 6\,H_2O \qquad E^0 = 2.11\,V, \tag{19.}$$

than a hydrogen fuel cell, as well as high efficiency (75%) and extremely high energy density (theoretical 2,580 Wh kg^{-1}, experimentally demonstrated greater than 1,000 Wh kg^{-1}, predicted

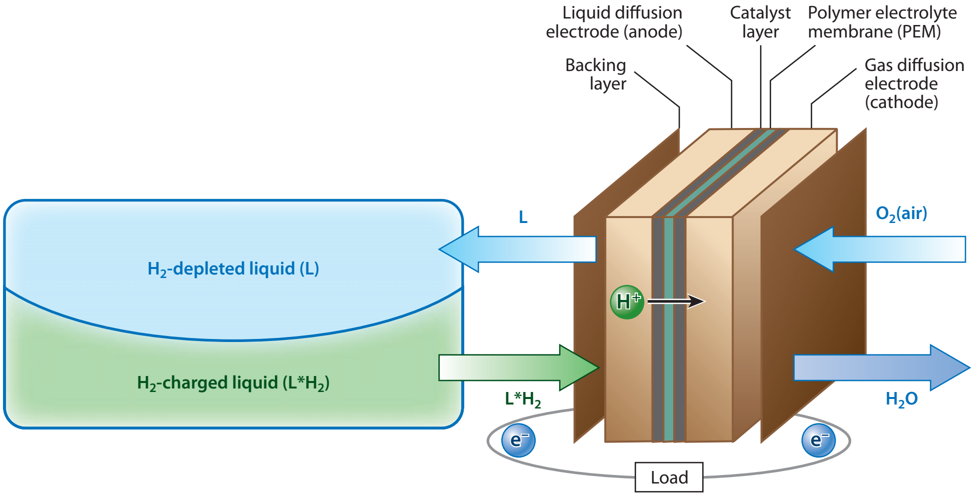

Figure 2

Direct organic fuel cell/flow battery concept.

practical 200 Wh kg^{-1}) (139, 140). The claimed reaction reversibility that would make this system suitable for EES (140) needs to be demonstrated on both cathode and anode sides. However, a recent study showed that electrosynthesis of $NaBH_4$ from $NaBO_2$ is difficult (141).

A novel RFC concept, a direct organic fuel cell/flow battery that uses a hydrogen-rich organic liquid as a reversible fuel in an electrochemical cell, has been proposed (142, 143). In this concept (**Figure 2**), in the discharge mode the organic liquid is fed directly to the anode of a PEM fuel cell, where it is electrochemically dehydrogenated to form a stable, hydrogen-depleted organic compound without ever generating gaseous H_2 to produce power. In the charge mode, water is electrolyzed to hydrogenate the spent liquid back to the starting liquid compound (Equation 20):

$$L^*nH_2 + n/2\ O_2 \Leftrightarrow L + n\ H_2O \qquad E^0 = 1.0{-}1.1\ V. \qquad 20.$$

The system works as a hybrid of a fuel cell and a flow battery. An example of such an organic liquid fuel is decalin, which can be oxidatively dehydrogenated to naphthalene to produce 10 protons and 10 electrons that, taking into account decalin's molecular weight of 128.17, makes it an anode material with specific energy density only approximately two times less than lithium metal. The theoretical energy density of the organic liquid-oxygen couple may reach 1,350 Wh kg^{-1}, approximately 20–40 times higher than that of common flow batteries. As other examples, electrochemical dehydrogenation of cyclohexane vapor in a PEM fuel cell has been demonstrated (144, 145), and electrocatalytic hydrogenation of aromatic compounds is also known (146).

To make this concept a reality, an effective hydrogenation/dehydrogenation electrocatalyst, a low-humidity PEM, and a compatible high–energy density organic fuel should be developed. To solve these challenging problems, a DOE-funded Energy Frontier Research Center on Electrocatalysis, Transport Phenomena, and Materials has been created (**http://ge.geglobalresearch.com/technologies/chemical-technologies-materials-characterization/efrc/**).

COMPARISON OF ELECTROCHEMICAL ENERGY STORAGE SYSTEMS

Growing energy demand will drive a substantial increase in the installed electricity generation capacity (up to 77% by 2030) and a corresponding increase in EES capacity (147). It is estimated that the United States alone will need to build, in the next few years, approximately 13 GW of EES systems to support the grid, and evidently even more when the increasing share of intermittent renewable sources is taken into account. The most important parameters that will determine successful deployment of electrochemical EES systems are cost, reliability, robustness, flexibility, and environmental impact. Another factor is availability of electroactive materials. For example, mass production of electric cars might strain the lithium supply and make it less available for stationary applications. Estimates of global extractable lithium reserves vary from 13.4 million metric tons by Tahil (148) to a more optimistic 28.4 million tons by Keith Evans (149). These reserves are more than enough to provide Li-ion batteries for the whole global fleet of cars. However, for much larger scale stationary storage, lithium availability may be a problem.

Electrochemical EES technologies have several advantages compared with other options. Pumped hydro and CAES have advantages for large-scale storage, but they are location specific and, therefore, cannot be used in many places. They also suffer from high energy transmission costs.

According to a recent cost analysis (**Table 2**), redox flow batteries and sodium nickel chloride batteries are the least expensive for energy applications, whereas Li-ion batteries may be preferred for high power applications. Clearly, no single technology is equally suitable for all applications, or even for the same application in different locations. Case-by-case analysis should be performed to select the best EES option.

The best choice within electrochemical EES depends on scale and application. For example, Li-ion batteries are best for smaller scale power applications, whereas redox flow batteries are more appropriate than secondary batteries for large-scale energy applications. Molten sodium batteries, especially the promising Na-$NiCl_2$ batteries, could be used in the intermediate scale (kW to MW).

Secondary batteries with solid active materials have a fundamental problem of the thermodynamic instability of their complex 3D electrode structures owing to material expansion/contraction, reaction with electrolyte, and stratification due to different densities; this instability leads to an unavoidable degradation of electrodes and capacity loss. Reducing the size

Table 2 Technical and economic parameters of batteries for electric energy storage (148)

Technology	Specific energy, Wh kg^{-1}		Specific power, W kg^{-1}	Round trip efficiency, %	Self-discharge, % day^{-1}	Cycle life	Power cost, \$ kW^{-1}	Energy cost, \$ kWh^{-1}
	Theory	Practical						
VRLA	170	30–50	75–300	70–80	0.1–0.3	500–1,000	300–600	200–400
NiCd	315	50–75	150–300	60–70	0.2–0.6	2,000–2,500	500–1,500	800–1,500
NAS	755	150–240	150–230	75–90[a]	0	2,500	1,000–3,000	300–500
$NaNiCl_2$	790	100–120	150–200	85–90[a]	0	2,500+	150–300	100–200
Li-ion	560	75–200	150–315	85–98	0.1–0.3	1,000–10,000	175–4,000	500–2,500
Zinc-bromine	217	30–50	–	65–75	Small	2,000+	700–2,500	150–1,000
VRB	34	10–25	–	75–85	Small	12,000	600–1,500	150–1,000

[a] Total efficiency is 5–7% lower owing to heat losses to maintain cell operating temperatures.

Abbreviations: VRLA, valve-regulated lead-acid; NAS, sodium-sulfur; VRB, vanadium redox battery of particles, using composite cathodes and anodes, designing support scaffolds, and optimizing porosity effectively may reduce the degradation rate but cannot eliminate it.

Li-ion batteries with high power and energy density are under intensive study for mobile applications and are under consideration for stationary applications. However, they have many disadvantages (high cost, limited lifetime, restricted electrode thickness that complicates the cell design, temperature sensitivity, and safety) that should be addressed before large-scale implementation in stationary EES. To address major challenges, research is focused on the design of inexpensive cathode materials with low expansion and increased capacity (e.g., multielectron materials such as transition metal fluorides), electrolytes with improved safety and conductivity (e.g., aqueous electrolytes), new anode materials, and improved protection and plating of lithium metal. The scalability of Li-ion batteries to large EES units will present additional challenges.

Molten sodium batteries are well positioned for intermediate (up to MW)-scale EES. Sodium metal chloride batteries are safer than NAS batteries and can deliver more power. These batteries are independent of ambient temperature and have high efficiency and zero self-discharge, but energy must be spent to compensate for heat loss during idle periods. This may be not an issue if these batteries are used continuously, e.g., in hybrid telecom applications. Their major disadvantage is low power, for example, relative to Li-ion batteries. To increase power, new designs, novel electrolytes, and sodium-conducting materials need to be explored. The battery cost can be further reduced through development of inexpensive cathode materials and by increases in production volume.

The regenerative hydrogen-oxygen fuel cells, coupled with even current hydrogen storage, have by far the highest energy density (450–800 Wh kg^{-1}) (150), more than 2–3 times that forecast for any secondary batteries. They also have low environmental impact and are easily scalable but suffer from low round-trip energy efficiency, high catalyst and membrane cost, ineffective hydrogen storage, and slow transition from charge to discharge. Round trip efficiency of regenerative fuel cells depends on the efficiencies of both fuel cell and electrolyzer operations. The theoretical efficiency of the hydrogen PEM fuel cell ($\varepsilon = \Delta G/\Delta H$) is 84%, and that of a PEM electrolyzer is 93% at reasonable cell potentials (151), which gives an overall efficiency of 78%. The real efficiency of an RFC is much lower, as small as approximately 40%, owing mostly to the ORR overpotential (152). If oxygen is not recuperated, this value is reduced to 26% (153). Replacement of oxygen with other oxidants, e.g., bromine, eliminates the ORR issue but introduces the problems of corrosion and toxicity. Substitution of stored hydrogen with organic liquids with high energy density (142, 143) may be promising, but the fundamental problems in developing electrocatalysts and low-humidity membranes need to be solved.

Flow redox batteries are better suited for large-scale applications. They have high efficiency, are easily scalable, and may be fully discharged and charged without overcharging. In addition, they may be instantly charged by mechanical replacement of discharged electrolytes with charged ones. The main problems of flow batteries are low energy density, short membrane lifetime, complex plumbing, and pumping that could lead to leaks of corrosive and toxic materials. It seems that the current trend in flow battery deployment is to build modular kW-scale systems that can be scaled up by combining the required number of independent systems rather than simply to increase the electrolyte tank size. Such systems are more resilient because the failure of one module will result in minimal loss of capacity, and maintenance and electrolyte replacement is less expensive. Comparative analysis of these flow cells showed that vanadium/vanadium batteries are superior to zinc/bromine batteries (toxic bromine, corrosion) and iron/chromium batteries (low capacity retention because of electrolyte crossover) (154). To increase energy density and efficiency, research will need to target new electroactive materials and ion-selective membranes that effectively stop transport of redox materials but maintain high a flux of ions and water.

CONCLUSIONS

To be competitive with other energy storage options, the capital cost of electrochemical EES should be decreased and the cycle life and reliability increased. This will define future research and development in the electrochemical EES area.

Currently, lead-acid (VRLA and flooded) batteries are the most frequently used in all types of stationary applications. However, other emerging electrochemical technologies likely will soon meet and exceed the required technical specifications and challenge lead-acid batteries in this market (155). The most promising technologies in the short term are high-temperature sodium batteries with β''-alumina electrolyte, Li-ion batteries, and flow batteries. In the long run, assuming further technical advances, regenerative fuel cells and lithium metal batteries with high energy densities may obtain substantial market share.

DISCLOSURE STATEMENT

The author is a General Electric Global Research employee and a director of the Energy Frontier Research Center funded by the U.S. Department of Energy, Office of Basic Energy Sciences, which might be perceived as affecting the objectivity of this review.

ACKNOWLEDGMENTS

The author would like to thank Drs. G. Merfeld, R. Perry, J. Rijssenbeek, and G. Zappi for help in manuscript preparation and helpful discussions. This material is based on work supported as part of the Center for Electrocatalysis, Transport Phenomena, and Materials (CETM) for Innovative Energy Storage, an Energy Frontier Research Center funded by the U.S. Department of Energy, Office of Science, Office of Basic Energy Sciences under Award Number DE-SC00001055.

LITERATURE CITED

1. Walawalkar R, Apt J. 2008. Market analysis of emerging electric energy storage systems. *Rep. DOE/NETL-2008/1330*, Carnegie Mellon University, Pittsburgh, Penn.
2. Haas OJ, Cairns E. 1999. Chapter 6. Electrochemical energy storage. *Annu. Rep. Prog. Chem. Sect. C* 95:163–98
3. Beck F, Ruetschi P. 2000. Rechargeable batteries with aqueous electrolytes. *Electrochim. Acta* 45:2467–82
4. Ponce de Leon C, Frias-Ferrer A, Gonzalez-Garcia J, Szanto DA, Walsh FC. 2006. Redox flow cells for energy conversion. *J. Power Sources* 160:716–32
5. Ibrahim H, Ilinca A, Perron J. 2008. Energy storage systems—characteristics and comparisons. *Renew. Sustain. Energy Rev.* 12:1221–50
6. Chen H, Cong TN, Yang W, Tan C, Li Y, Ding Y. 2009. Progress in electrical energy storage system: a critical review. *Prog. Nat. Sci.* 19:291–312
7. Oudalov A, Buehler T, Chartouni D. 2008. *Utility scale application of energy storage*. Presented at IEEE Energy 2030, Atlanta, GA
8. Electric Power Research Institute. 2006. Technology review and assessment of distributed energy resources: distributed energy storage. *Rep. 1012983*, Palo Alto, CA
9. Baque L. 2004. Comparison of energy storage systems applicables to sustainable use of energy. *Proc. World Renew. Energy Congr. VIII: Link. World Renew. Energy, 8th*, Denver, CO, pp. 198–202. Golden, CO: Natl. Renew. Energy Lab.
10. Butler PC. 1994. Battery energy storage for utility applications: Phase I—opportunities analysis. *Rep. SAND94-2605*, Sandia Natl. Lab., Albuquerque
11. Pike Research. 2010. *Energy storage on the grid*. **http://www.pikeresearch.com/research/energy-storage-on-the-grid**

12. Dell RM, Rand DAJ. 2001. Energy storage—a key technology for global energy sustainability. *J. Power Sources* 100:2–17
13. Lam LT, Furukawa J. 2010. *U.S. Patent Application No. 2010/0,203,362*
14. Lam LT, Furukawa J, Takada T, Monma D, Kanou T. 2010. *U.S. Patent Application No. 2010/0,175,934*
15. Buiel ER, Cole JE. 2009. *U.S. Patent Application No. 2009/0,103,242*
16. Commonw. Sci. Ind. Res. Org. 2010. *UltraBattery: no ordinary battery*. **http://www.csiro.au/science/Ultra-Battery.html**
17. Kelley KC, Votoupal JJ. 2005. *U.S. Patent No. 6,979,513*
18. Kelley KC, Taylor SC. 2006. *U.S. Patent No. 7,105,252*
19. Klebanov LN, Hansen CP, Wynn DA, Trischan GM, Schaeffer CJ. 2001. *U.S. Patent No. 6,300,007*
20. Toniazzo V. 2006. The key to success: gelled-electrolyte and optimized separators for stationary lead-acid batteries. *J. Power Sources* 158:1124–32
21. An SY, Jeong ED, Won MS, Shim YB. 2008. The optimization of gel electrolytes on performance of valve regulated lead acid batteries. *Bull. Korean Chem. Soc.* 29:998–1002
22. Tang Z, Wang J, Mao X-x, Shao H, Chen Q, et al. 2007. Investigation and application of polysiloxane-based gel electrolyte in valve-regulated lead-acid battery. *J. Power Sources* 168:49–57
23. Zelinsky M, Koch J, Fetcenko M. 2010. Heat tolerant nimh batteries for stationary power. *Proc. 2010 Battcon Station. Battery Conf., Orlando*, pp. 12-1–12-6. Pompano Beach, FL: Battcon/Albercorp
24. Jurczyk M, Smardz L, Smardz K, Nowak M, Jankowska E. 2003. Nanocrystalline $LaNi_5$-type electrode materials for Ni-MH_x batteries. *J. Solid State Chem.* 171:30–37
25. Ovshinsky SR, Fetcenko MA. 2001. Development of high catalytic activity disordered hydrogen-storage alloys for electrochemical application in nickel-metal hydride batteries. *Appl. Phys. A* 72:239–44
26. Young K, Fetcenko MA, Koch J, Morii K, Shimizu T. 2009. Studies of Sn, Co, Al, and Fe additives in C14/C15 Laves alloys for NiMH battery application by orthogonal arrays. *J. Alloys Compd.* 486:559–69
27. Vassal N, Salmon E, Fauvarque J-F. 1999. Nickel metal hydride rechargeable batteries with polymer electrolytes. *Rev. Electr. Electron.* 1999:79–851 (In French)
28. Lu X, Xia G, Lemmon JP, Yang Z. 2010. Advanced materials for sodium-beta alumina batteries: Status, challenges and perspectives. *J. Power Sources* 195:2431–42
29. Virkar AV, Jue JF, Fung KZ. 2003. *U.S. Patent No. 6,537,940*
30. Virkar AV. 2008. A high temperature electrochemical energy storage system based on sodium β''-alumina solid electrolyte (BASE). *Rep. DE-FC26-05NT42623*, Univ. of Utah, Salt Lake City
31. Wen Z, Cao J, Gu Z, Xu X, Zhang F, Lin Z. 2008. Research on sodium sulfur battery for energy storage. *Solid State Ionics* 179:1697–701
32. Park C-W, Ahn J-H, Ryu H-S, Kim K-W, Ahn H-J. 2006. Room-temperature solid-state sodium/sulfur battery. *Electrochem. Solid-State Lett.* 9:A123–25
33. Ryu DH, Park CW, Ahn HJ, Kim BJ, Lee EM, et al. 2007. *U.S. Patent Application No. 2007/0,154,814*
34. Linden D, Reddy TB. 2002. *Handbook of Batteries*. New York: McGraw-Hill. 3rd ed.
35. Scrosati B, Garche J. 2010. Lithium batteries: status, prospects and future. *J. Power Sources* 195:2419–30
36. Padhi AK, Nanjundaswamy KS, Goodenough JB. 1997. Phospho-olivines as positive-electrode materials for rechargeable lithium batteries. *J. Electrochem. Soc.* 144:1188–94
37. Chung S-Y, Bloking JT, Chiang Y-M. 2002. Electronically conductive phospho-olivines as lithium storage electrodes. *Nat. Mater.* 1:123–28
38. Guerfi A, Sévigny S, Lagacé M, Hovington P, Kinoshita K, Zaghib K. 2003. Nano-particle $Li_4Ti_5O_{12}$ spinel as electrode for electrochemical generators. *J. Power Sources* 119–121:88–94
39. Aurbach D, Talyosef Y, Markovsky B, Markevich E, Zinigrad E, et al. 2004. Design of electrolyte solutions for Li and Li-ion batteries: a review. *Electrochim. Acta* 50:247–54
40. Frankhouser J, Anderson J, Boyer D. 2010. Commercial lithium-ion reserve power systems. *Proc. 2010 Battcon Station. Battery Conf., Orlando*, pp. 4-1–4-10, Pompano Beach, FL: Battcon/Albercorp.
41. Coetzer J, Galloway RC, Bones RJ, Teagle DA, Moseley PT. 1983. *DE Patent No. 3,245,812*
42. Iacovangelo CD, Bogdan DC Jr, Tysoe SA, Vallance MA, Zappi GD, et al. 2009. *U.S. Patent No. 7,632,604*

43. Vallance MA, Bogdan D, Seshadri HN, Gourishankar KV, Sundararajan G, Iacovangelo CD. 2010. *U.S. Patent Application No. 2010/0,062,334*
44. Bohm H, Beyermann G. 1999. ZEBRA batteries, enhanced power by doping. *J. Power Sources* 84:270–74
45. Turconi A. 2007. *Developments and improvements in ZEBRA® nickel sodium chloride batteries*. Presented at Electric Vehicle Symposium EVS23, Anaheim , CA
46. Bones RJ, Teagle DA, Brooker SD, Cullen FL. 1989. Development of a nickel/nickel dichloride positive electrode for a liquid sodium (ZEBRA) battery cell. *J. Electrochem. Soc.* 136:1274–77
47. Ratnakumar BV, Surampudi S, Halpert G. 1994. Effects of sulfur additive on the performance of Na/$NiCl_2$ cells. *J. Power Sources* 48:349–60
48. Prakash J, Redey L, Vissers D. 2000. Effect of chemical additives on the performance of Na/$NiCl_2$ cells. *Ionics* 6:210–17
49. Prakash J, Redey L, Vissers DR, DeGruson J. 2000. Effect of sodium iodide additive on the electrochemical performance of sodium/nickel chloride cells. *J. Appl. Electrochem.* 30:1229–33
50. Sudworth JL. 2001. The sodium/nickel chloride (ZEBRA) battery. *J. Power Sources* 100:149–63
51. Galloway RC, Haslam S. 1999. The ZEBRA electric vehicle battery: power and energy improvements. *J. Power Sources* 80:164–70
52. Bourgeois R. 2010. Sodium-metal halide batteries for stationary applications. *Proc. 2010 Battcon Station. Battery Conf., Orlando*, pp. 11-1–11-6. Pompano Beach, FL: Battcon/Albercorp
53. Gaillac L, Skaggs D, Pinsky N. 2006. *Sodium nickel chloride battery performance in a stationary application*. Presented at Annu. Intl. Telecommun. Energy Conf., 28th, Providence
54. Li W, Dahn JR, Wainwright DS. 1994. Rechargeable lithium batteries with aqueous electrolytes. *Science* 264:1115–18
55. Luo J-Y, Cui W-J, He P, Xia Y-Y. 2010. Raising the cycling stability of aqueous lithium-ion batteries by eliminating oxygen in the electrolyte. *Nat. Chem.* 2:760–65
56. Badway F, Pereira N, Cosandey F, Amatucci GG. 2003. Carbon-metal fluoride nanocomposites. *J. Electrochem. Soc.* 150:A1209–18
57. Li H, Balaya P, Maier J. 2004. Li-storage via heterogeneous reaction in selected binary metal fluorides and oxides. *J. Electrochem. Soc.* 151:A1878–85
58. Cabana J, Monconduit L, Larcher D, Palacín MR. Beyond intercalation-based Li-ion batteries: the state of the art and challenges of electrode materials reacting through conversion reactions. *Adv. Mater.* 22:E170–92
59. Girishkumar G, McCloskey B, Luntz AC, Swanson S, Wilcke W. 2010. Lithium-air battery: promise and challenges. *J. Phys. Chem. Lett.* 1:2193–203
60. Zhang T, Imanishi N, Shimonishi Y, Hirano A, Takeda Y, et al. 2010. A novel high energy-density rechargeable lithium/air battery. *Chem. Commun.* 46:1661–63
61. Visco SJ, Katz BD, Nimon YS, De Jonghe LC. 2007. *U.S. Patent No. 7,282,295*
62. Hayashi A, Ohtomo T, Mizuno F, Tadanaga K, Tatsumisago M. 2003. All-solid-state Li/S batteries with highly conductive glass-ceramic electrolytes. *Electrochem. Commun.* 5:701–5
63. Eitouni HB, Singh M. 2010. *U.S. Patent Application No. 2010/0,227,224*
64. Edman L, Doeff MM, Ferry A, Kerr J, De Jonghe LC. 2000. Transport properties of the solid polymer electrolyte system $P(EO)_n$LiTFSI. *J. Phys. Chem. B* 104:3476–80
65. Singh M, Odusanya O, Wilmes GM, Eitouni HB, Gomez ED, et al. 2007. Effect of molecular weight on the mechanical and electrical properties of block copolymer electrolytes. *Macromolecules* 40:4578–85
66. Wang Y, Zhou H. 2010. A lithium-air battery with a potential to continuously reduce O_2 from air for delivering energy. *J. Power Sources* 195:358–61
67. Cheng H, Scott K. 2010. Carbon-supported manganese oxide nanocatalysts for rechargeable lithium-air batteries. *J. Power Sources* 195:1370–74
68. Kumar B, Kumar J, Leese R, Fellner JP, Rodrigues SJ, Abraham KM. 2010. A solid-state, rechargeable, long cycle life lithium-air battery. *J. Electrochem. Soc.* 157:A50–54
69. Li H, Wang Y, Na H, Liu H, Zhou H. 2009. Rechargeable Ni-Li battery integrated aqueous/non-aqueous system. *J. Am. Chem. Soc.* 131:15098–99

70. Mikhaylik Y. 2006. *Fundamental chemistry of Sion power Li/S battery*. Presented at Intl. Battery Assoc. Hawaii Battery Conf., Waikoloa, HI
71. Mikhaylik YV, Akridge JR. 2004. Polysulfide shuttle study in the Li/S battery system. *J. Electrochem. Soc.* 151:A1969–76
72. Kolosnitsyn VS, Karaseva EV, Amineva NA, Batyrshina GA. 2002. Cycling lithium-sulfur batteries. *Russ. J. Electrochem.* 38:329–31
73. Kolosnitsyn VS, Karaseva EV. 2008. Lithium-sulfur batteries: problems and solutions. *Russ. J. Electrochem.* 44:506–9
74. Ryu H-S, Ahn H-J, Kim K-W, Ahn J-H, Lee J-Y. 2006. Discharge process of Li/PVDF/S cells at room temperature. *J. Power Sources* 153:360–64
75. Choi J-W, Kim J-K, Cheruvally G, Ahn J-H, Ahn H-J, Kim K-W. 2006. Rechargeable lithium/sulfur battery with suitable mixed liquid electrolytes. *Electrochim. Acta* 52:2075–82
76. Mikhaylik Y, Kovalev I, Xu J, Schock R. 2008. Rechargeable Li-S battery with area specific resistance (ASR) 350 Wh/kg and specific power 3000 W/kg. *ECS Trans.* 13:53–59
77. Yang Y, McDowell MT, Jackson A, Cha JJ, Hong SS, Cui Y. New nanostructured Li_2S/silicon rechargeable battery with high specific energy. *Nano Lett.* 10:1486–91
78. Friesen CA, Buttry DA. 2010. *U.S. Patent Application No. 2010/0,285,375*
79. Watarai A, Kubota K, Yamagata M, Goto T, Nohira T, et al. 2008. A rechargeable lithium metal battery operating at intermediate temperatures using molten alkali bis(trifluoromethylsulfonyl)amide mixture as an electrolyte. *J. Power Sources* 183:724–29
80. Shimotake H, Johnson CE, Foster MS, Cairns EJ. 1970. *U.S. Patent No. 3,488,221*
81. Fischer AK, Maroni VA, Tevebaugh AD, Cairns EJ. 1970. *U.S. Patent No. 3,531,324*
82. Sadoway D, Ceder G, Bradwell D. 2008. *U.S. Patent Application No. 2008/0,044,725*
83. Skyllas-Kazacos M, Kazacos G, Poon G, Verseema H. 2010. Recent advances with UNSW vanadium-based redox flow batteries. *Int. J. Energy Res.* 34:182–89
84. Skyllas Kazacos M, Rychick M, Robins R. 1988. *U.S. Patent No. 4,786,567*
85. Luo Q, Zhang H, Chen J, Qian P, Zhai Y. 2008. Modification of Nafion membrane using interfacial polymerization for vanadium redox flow battery applications. *J. Membr. Sci.* 311:98–103
86. Zeng J, Jiang C, Wang Y, Chen J, Zhu S, et al. 2008. Studies on polypyrrole modified Nafion membrane for vanadium redox flow battery. *Electrochem. Commun.* 10:372–75
87. Xi J, Wu Z, Teng X, Zhao Y, Chen L, Qiu X. 2008. Self-assembled polyelectrolyte multilayer modified Nafion membrane with suppressed vanadium ion crossover for vanadium redox flow batteries. *J. Mater. Chem.* 18:1232–38
88. Qiu J, Zhai M, Chen J, Wang Y, Peng J, et al. 2009. Performance of vanadium redox flow battery with a novel amphoteric ion exchange membrane synthesized by two-step grafting method. *J. Membr. Sci.* 342:215–20
89. Chen D, Wang S, Xiao M, Meng Y. 2010. Preparation and properties of sulfonated poly(fluorenyl ether ketone) membrane for vanadium redox flow battery application. *J. Power Sources* 195:2089–95
90. Chakrabarti MH, Lindfield Roberts EP, Saleem M. 2010. Charge-discharge performance of a novel undivided redox flow battery for renewable energy storage. *Int. J. Green Energy* 7:445–60
91. Kondo S, Tokuda N. 2002. *JP Patent No. 2,002,216,833*
92. Rydh CJ. 1999. Environmental assessment of vanadium redox and lead-acid batteries for stationary energy storage. *J. Power Sources* 80:21–29
93. Tokuda N, Kanno T, Hara T, Shigematsu T, Tsustsui Y, et al. 2000. Development of a redox flow battery system. *SEI Technical Review* 50:88–94
94. Remick RJ, Ang PGP. 1984. *U.S. Patent No. 4,485,154*
95. Zhao P, Zhang H, Zhou H, Yi B. 2005. Nickel foam and carbon felt applications for sodium polysulfide/bromine redox flow battery electrodes. *Electrochim. Acta* 51:1091–98
96. Zito R. 1997. *U.S. Patent No. 5,612,148*
97. Kautek W, Conradi A, Sahre M, Fabjan C, Drobits J, et al. 1999. In situ investigations of bromine-storing complex formation in a zinc-flow battery at gold electrodes. *J. Electrochem. Soc.* 146:3211–16
98. Winter R. 2010. *U.S. Patent Application No. 2010/0,021,805*

99. Clarke RL, Dougherty B, Harrison S, Millington PJ, Mohanta S. 2009. *U.S. Patent No. 7,625,663*
100. Clarke RL, Dougherty B, Harrison S, Millington JP, Mohanta S. 2009. *U.S. Patent No. 7,560,189*
101. Thaller LH. 1976. *U.S. Patent No. 3,996,064*
102. Thaller LH. 1979. Redox flow cell energy storage systems *NASA Rep. AIAA PAPER 79–0989*, Glenn Res. Cent., Cleveland, Ohio
103. Gahn RF, Hagedorn NH, Johnson JA. 1985. Cycling performance of the iron-chromium redox energy storage system. *Rep. NASA-TM-87034*, Glenn Research Center, Cleveland, Ohio
104. Garces P, Climent MA, Aldaz A. 1987. Systems for storage of electric energy. I. First results of an iron-chromium redox battery. *An. Quim. Ser. A* 83:9–11
105. Climent MA, Garces P, Lopez-Segura M, Aldaz A. 1987. Systems for storage of electric energy. II. Filter press-type iron/chromium redox battery. *An. Quim. Ser. A* 83:12–14
106. Lopez-Atalaya M, Codina G, Perez JR, Vazquez JL, Aldaz A. 1992. Optimization studies on an iron/chromium redox flow battery. *J. Power Sources* 39:147–54
107. Johnson DA, Reid MA. 1985. Chemical and electrochemical behavior of the Cr(III)/Cr(II) half-cell in the iron-chromium redox energy storage system. *J. Electrochem. Soc.* 132:1058–62
108. Gahn RF, Hagedorn N. 1987. Negative-electrode catalysts for Fe/Cr redox cells. *Rep. NASA LEW-14028*, Glenn Res. Cent., Cleveland, Ohio
109. Bae CH, Roberts EPL, Dryfe RAW. 2002. Chromium redox couples for application to redox flow batteries. *Electrochim. Acta* 48:279–87
110. Vafiadis H, Skyllas-Kazacos M. 2006. Evaluation of membranes for the novel vanadium bromine redox flow cell. *J. Membr. Sci.* 279:394–402
111. Swartbooi A, Van Vuuren D. 2006. *Investigating improvements on redox flow batteries*. Presented at S. Afr. Chem. Eng. Congr., Durban.
112. Fang B, Iwasa S, Wei Y, Arai T, Kumagai M. 2002. A study of the Ce(III)/Ce(IV) redox couple for redox flow battery application. *Electrochim. Acta* 47:3971–76
113. Pletcher D, Wills R. 2004. A novel flow battery: a lead acid battery based on an electrolyte with soluble lead(II). Part II. Flow cell studies. *Phys. Chem. Chem. Phys.* 6:1779–85
114. Hazza A, Pletcher D, Wills R. 2004. A novel flow battery: a lead acid battery based on an electrolyte with soluble lead(II). Part I. Preliminary studies. *Phys. Chem. Chem. Phys.* 6:1773–78
115. Pletcher D, Wills R. 2005. A novel flow battery—a lead acid battery based on an electrolyte with soluble lead(II). III. The influence of conditions on battery performance. *J. Power Sources* 149:96–102
116. Hazza A, Pletcher D, Wills R. 2005. A novel flow battery—a lead acid battery based on an electrolyte with soluble lead(II). IV. The influence of additives. *J. Power Sources* 149:103–11
117. Pletcher D, Zhou H, Kear G, Low CTJ, Walsh FC, Wills RGA. 2008. A novel flow battery—a lead-acid battery based on an electrolyte with soluble lead(II): Part VI. Studies of the lead dioxide positive electrode. *J. Power Sources* 180:630–34
118. Li X, Pletcher D, Walsh FC. 2009. A novel flow battery: a lead acid battery based on an electrolyte with soluble lead(II): Part VII. Further studies of the lead dioxide positive electrode. *Electrochim. Acta* 54:4688–95
119. Wills RGA, Collins J, Stratton-Campbell D, Low CTJ, Pletcher D, Walsh FC. 2010. Developments in the soluble lead-acid flow battery. *J. Appl. Electrochem.* 40:955–65
120. Collins J, Li X, Pletcher D, Tangirala R, Stratton-Campbell D, et al. 2010. A novel flow battery: a lead acid battery based on an electrolyte with soluble lead(II). Part IX: electrode and electrolyte conditioning with hydrogen peroxide. *J. Power Sources* 195:2975–78
121. Yamamura T, Shiokawa Y, Yamana H, Moriyama H. 2002. Electrochemical investigation of uranium β^2-diketonates for all-uranium redox flow battery. *Electrochim. Acta* 48:43–50
122. Yamamura T, Shirasaki K, Shiokawa Y, Nakamura Y, Kim SY. 2004. Characterization of tetraketone ligands for active materials of all-uranium redox flow battery. *J. Alloys Compd.* 374:349–53
123. Xue FQ, Wang YL, Wang WH, Xin-Dong W. 2008. Investigation on the electrode process of the Mn(II)/Mn(III) couple in redox flow battery. *Electrochimica Acta* 53:6636–42
124. Wen YH, Zhang HM, Qian P, Zhou HT, Zhao P, et al. 2006. A study of the Fe(III)/Fe(II)-triethanolamine complex redox couple for redox flow battery application. *Electrochim. Acta* 51:3769–75

125. Wen YH, Zhang HM, Qian P, Zhou HT, Zhao P, et al. 2006. Studies on iron (Fe^{3+}/Fe^{2+})-complex/bromine (Br_2/Br^-) redox flow cell in sodium acetate solution. *J. Electrochem. Soc.* 153:A929–34
126. Modiba P, Crouch AM. 2008. Electrochemical study of cerium(IV) and its complexes with ethylenediaminetetraacetic acid (EDTA) and diethylenetriaminepentaacetate (DTPA) ligands as potential electrolytes for redox flow batteries. *Proc. Power Sources Conf.*, 43rd, Philadelphia, Pennsylvania, pp. 71–72. Army Communications-Electronics Command, Fort Monmouth, NJ.
127. Cheng J, Zhang L, Yang Y-S, Wen Y-H, Cao G-P, Wang X-D. 2007. Preliminary study of single flow zinc-nickel battery. *Electrochem. Commun.* 9:2639–42
128. Pan J, Sun Y, Cheng J, Wen Y, Yang Y, Wan P. 2008. Study on a new single flow acid Cu-PbO_2 battery. *Electrochem. Commun.* 10:1226–29
129. Findl E, Klein M. 1967. Electrolytically regenerative hydrogen/oxygen fuel cell battery. In *Regenerative EMF Cells*, *Advances in Chemistry Series*, ed. CE Crouthamel, HL Recht, 64:292–305. Washington, D.C.: American Chemical Society
130. Barbir F, Dalton L, Molter T. 2003. *Regenerative fuel cells for energy storage: efficiency and weight trade-offs*. Presented at Intl. Energy Convers. Eng. Conf., 1st, Portsmouth, VA
131. Wang T, Wei C. 2007. *U.S. Patent No. 7,282,294*
132. Yang H, Huang Q, Chang W, Cai J, Liu J, et al. 2007. *WO Patent No. 2,007,075,721*
133. Cai J, Wei C, Huang Q, Liu J, Yang H, et al. 2008. *U.S. Patent Application No. 2008/0,145,737*
134. Choi B, Lee S, Fushimi C, Tsutsumi A. 2009. Development of NiMH-based fuel cell/battery (FCB) system: characterization of $Ni(OH)_2/MnO_2$ positive electrode for FCB. *J. Power Sources* 194:1150–55
135. Kosek JA, LaConti AB. 1984. Investigation of bromine complexed hydrogen/bromine regenerative fuel cells for portable electric power. *Rep. MERDC-38*, General Electric Co., Wilmington, Mass.
136. Parker R, Clapper WLJ. 2001. Hydrogen-based utility energy storage system. NREL/CP-570–30535. *Proc. DOE Hydrog. Program Merit Rev.* **http://www1.eere.energy.gov/hydrogenandfuelcells/pdfs/30535ag.pdf**
137. Livshits V, Ulus A, Peled E. 2006. High-power H_2/Br_2 fuel cell. *Electrochem. Commun.* 8:1358–62
138. Disselkamp RS. 2008. Energy storage using aqueous hydrogen peroxide. *Energy Fuels* 22:2771–74
139. Choudhury NA, Raman RK, Sampath S, Shukla AK. 2005. An alkaline direct borohydride fuel cell with hydrogen peroxide as oxidant. *J. Power Sources* 143:1–8
140. Miley GH, Luo N, Mather J, Burton R, Hawkins G, et al. 2007. Direct $NaBH_4/H_2O_2$ fuel cells. *J. Power Sources* 165:509–16
141. Santos DMF, Sequeira CAC. 2010. On the electrosynthesis of sodium borohydride. *Int. J. Hydrog. Energy* 35:9851–61
142. Soloveichik GL, Lemmon JP, Zhao J-C. 2008. *U.S. Patent No. 2008/0,248,339*
143. Crabtree RH. 2008. Hydrogen storage in liquid organic heterocycles. *Energy Environ. Sci.* 1:134–38
144. Kariya N, Fukuoka A, Ichikawa M. 2003. Zero-CO_2 emission and low-crossover "rechargeable" PEM fuel cells using cyclohexane as an organic hydrogen reservoir. *Chem. Commun.* 2003:690–91
145. Kariya N, Fukuoka A, Ichikawa M. 2006. Direct PEM fuel cell using organic chemical hydrides with zero-CO_2 emission and low-crossover. *Phys. Chem. Chem. Phys.* 8:1724–30
146. Robin D, Comtois M, Martel A, Lemieux R, Cheong AK, et al. 1990. Electrocatalytic hydrogenation of organic compounds. IV. The electrocatalytic hydrogenation of fused polycyclic aromatic compounds at Raney nickel electrodes: the influence of catalyst activation and electrolysis conditions. *Can. J. Chem.* 68:1218–27
147. Energy Inf. Admin. 2010. *Annual energy outlook 2011 early release overview*. **http://www.eia.gov/forecasts/aeo/**
148. Tahil W. 2006. *The Trouble with Lithium*. Martainville, Fr.: Meridian Intl. Res.
149. Evans RK. 2008. *Lithium abundance—world lithium reserve*. **http://lithiumabundance.blogspot.com**
150. Burke KA. 1999. High energy density regenerative fuel cell systems for terrestrial applications. *NASA Rep. TM-1999–209429*, Glenn Res. Cent., Cleveland, Ohio
151. Papagiannakis I. 2005. *Studying and improving the efficiency of water electrolysis using a proton exchange membrane electrolyser*. MSc thesis. Strathclyde: Strathclyde Univ. 81 pp.

152. Chang B-j, Garcia CP, Johnson DW, Bents DJ, Scullin VJ, Jakupca IJ. 2005. Continuous operation of PEM regenerative fuel cell system for energy storage. *J. Fuel Cell Sci. Technol.* 4:497–500

153. Bernier E, Hamelin J, Agbossou K, Bose TK. 2005. Electric round-trip efficiency of hydrogen and oxygen-based energy storage. *Int. J. Hydrog. Energy* 30:105–11

154. Noack J, Tübke J. 2009. Redox flow energy storage for fluctuating renewable energies. *Proc. 2009 Battcon Station. Battery Conf., Orlando*, pp. 19-1–19-10. Pompano Beach, FL: Battcon/Albercorp

155. Perrin M, Saint-Drenan YM, Mattera F, Malbranche P. 2005. Lead-acid batteries in stationary applications: competitors and new markets for large penetration of renewable energies. *J. Power Sources* 144:402–10

Annual Review of Chemical and Biomolecular Engineering

Volume 2, 2011

Contents

Errata

An online log of corrections to *Annual Review of Chemical and Biomolecular Engineering* articles may be found at http://chembioeng.annualreviews.org/errata.shtml